computation

MDPI

Article

Improving the Accuracy of Infectious Disease Forecasts Based on Comparing Neural Network Architectures

Oleksandr Kovaliv [1], Yuriy Kondratenko [1,2], Ievgen Sidenko [1,*], Galyna Kondratenko [1] and Dmytro Chumachenko [3]

[1] Intellectual Information Systems Department, Petro Mohyla Black Sea National University, 68th Desantnykiv Str., 10, 54003 Mykolaiv, Ukraine; kizutoamazed@gmail.com (O.K.); yuriy.kondratenko@chmnu.edu.ua (Y.K.); halyna.kondratenko@chmnu.edu.ua (G.K.)
[2] Institute of Artificial Intelligence Problems, Mala Zhytomyrs'ka Str., 11/5, 01001 Kyiv, Ukraine
[3] Mathematical Modelling and Artificial Intelligence Department, National Aerospace University "Kharkiv Aviation Institute", Vadyma Manka Str., 17, 61070 Kharkiv, Ukraine; dichumachenko@gmail.com
* Correspondence: ievgen.sidenko@chmnu.edu.ua; Tel.: +380-93-88-37-915

Abstract

This paper aims to improve the accuracy of infectious disease forecasting using machine learning methods. The main results of this work are an analysis of infectious diseases spread in Ukraine during the time span from December 2016 to January 2024 and a performance comparison of different neural network architectures in the scope of time series forecasting. The following steps were taken: analysis of current forecasting methods, selection of neural network architectures, dataset preprocessing, and model testing. The developed system can be an effective tool for rational management decisions to ensure the epidemiological well-being and biosecurity of the population.

Keywords: infectious diseases; forecasting; time series; machine learning; neural networks

1. Introduction

Wars significantly amplify the spread of infectious diseases due to disrupted healthcare, reduced vaccination coverage, poor sanitation, and population displacement. Recent conflicts, such as in Syria and Yemen, have triggered major outbreaks of measles and cholera despite prior disease control. These examples highlight the critical need for robust epidemiological forecasting to predict infection dynamics and support timely public health interventions during wartime [1–3]. These include COVID-19, tuberculosis, viral hepatitis A, diarrhea, respiratory infections, HIV (human immunodeficiency virus), leishmaniasis, dengue fever, and many others [4–6]. The scientific literature provides numerous examples of how the conditions created by war facilitate the transmission of infectious diseases [7,8]. Therefore, the study of the conditions and risks of the spread of infections, the features of the manifestations of epidemic processes of infectious diseases can become the basis for the development of effective tools for adopting adequate situations and rational management decisions to ensure the epidemiological well-being and biosecurity of the population.

The main research objectives are the methods and technologies of time series forecasting, development and performance comparison of different neural network architectures that are most suitable for infectious disease spread predictions.

This study makes four main contributions. First, it compiles and carefully normalizes a national monthly dataset on 57 infectious diseases in Ukraine from December 2016 to January 2024, enabling consistent comparison across years and before/after the start of

Academic Editor: Ali Cemal Benim

Received: 27 October 2025
Revised: 17 February 2026
Accepted: 19 February 2026
Published: 21 February 2026

the full-scale war. Second, it provides a quantitative assessment of war-related changes in morbidity, showing that 22 diseases experienced an average increase of 62.38% in reported cases, while 35 diseases showed an average decrease of 35.52%. This analysis thus documents how cascading emergencies reshape the epidemic landscape. Third, it conducts a systematic empirical comparison of six advanced neural network architectures, RNN [9–15], Block RNN [16–22], N-BEATS [23–30], TCN [31–36], Transformer [28,32,37–40], and N-HiTS [41–43], under two training strategies (jointly on all time series vs. separately for each disease), using MAPE, MAE, and RMSE as evaluation metrics. Finally, the results demonstrate that training on multiple time series consistently improves accuracy compared to single-series training, suggesting informative cross-disease patterns, and N-BEATS achieves the best performance, while also highlighting the limits of all tested architectures on time series without clear seasonality, thereby outlining priorities for future model extensions.

The work aims to improve the accuracy of infectious disease forecasts based on comparing neural network architectures.

2. Related Works and Problem Statement

Long-horizon forecasting is critical in many important applications including risk management and planning [44,45]. Statistical modeling approaches, particularly those based on exponential smoothing and its various adaptations, are well-established and often serve as the default choice in industry. In healthcare, predictive monitoring of vital signs allows the detection of preventable adverse outcomes and application of life-saving interventions [44–47]. Let us consider some analogs of time series forecasting.

This study [46] presents a new two-dimensional epidemic prediction model that incorporates diffusion processes to account for spatial transmission—something most existing single-point, time-only models cannot do. The authors establish the model's mathematical soundness and introduce multiple parameterization schemes to better represent real-world factors influencing disease spread. Their results show that the model significantly improves predictions of both where and when infections occur. Applied to COVID-19 data, the model achieved regional average prediction scores of 76.5% for the July 2022 outbreak in Lanzhou and 70.7% for cases in China during May 2023. Overall, the study demonstrates that spatially aware modeling enhances understanding of epidemic dynamics and can support more effective public health planning.

This paper [47] introduces an extended SEIR model incorporating a vaccination compartment to simulate the spread of COVID-19 in Saudi Arabia. The model features seven infection stages: susceptible, exposed, infectious, quarantined, recovered, deaths, and vaccinated. A mathematical analysis is conducted to establish key properties such as non-negativity, boundedness, and the basic reproduction number of the model. To address uncertainties inherent in the model, the ensemble Kalman filter (EnKF) is employed to align model outputs and parameters with available data. The results demonstrate that the model can accurately predict epidemic developments over two-week periods and also explores the impact of vaccination on pandemic spread.

This study [48] focuses on developing and evaluating three statistical machine learning models—Random Forest, K-Nearest Neighbors, and Gradient Boosting—to predict COVID-19 incidence. The models were assessed for their predictive accuracy over 3, 7, 10, 14, 21, and 30-day periods, using data from Germany, Japan, South Korea, and Ukraine, chosen for their varying epidemic dynamics and control measures. The disadvantage of this study is that it is only focused on the COVID-19.

This study [49] proposes a probabilistic state-space model inspired by a susceptible-infectious-recovered (SIR) model to improve forecasting while addressing various uncer-

tainties. The authors demonstrate the effectiveness of their approach compared to other methods using multiple forecast accuracy metrics.

This study [50] aims to support global efforts against COVID-19 by applying artificial intelligence methods to real-time national data. It proposes a new predictive approach called the Exponential Smoothing Long Short-Term Memory (ESLSTM) model, which combines exponential smoothing with deep learning sequence networks to analyze daily trends in COVID-19 transmission and forecast the virus's short-term spread across countries. Using data from the Johns Hopkins dashboard, the model's performance is assessed through RMSE and R-squared metrics. Overall, the study highlights the potential of advanced machine learning and deep learning techniques to improve epidemic forecasting and provide actionable insights during a global health crisis.

This study [51] explores different deep learning and artificial neural network techniques, including Deep Belief Networks, AutoEncoders, and LSTM (Long short-term memory), to enhance power forecasting. Experiments were conducted using combinations of these algorithms to evaluate their forecasting capabilities against a standard multilayer perceptron (MLP) and a physical forecasting model for the energy output of 21 solar power plants. The results indicate that deep learning algorithms significantly outperform traditional artificial neural networks and other reference models, including physical models, in forecasting performance.

This paper [52] introduces a new electric load forecasting model that combines fuzzy time series (FTS) and a global harmony search algorithm (GHSA) with least squares support vector machines (LSSVM), referred to as the GHSA-FTS-LSSVM model. The approach begins by using the fuzzy c-means clustering (FCS) algorithm to determine the clustering centers for each group. The LSSVM then models the resulting series, which is optimized through the GHSA. To assess the model's effectiveness, real-world data from the Guangdong Province Industrial Development Database is utilized, with results compared to the autoregressive integrated moving average (ARIMA) model and other LSSVM hybrids such as genetic algorithm (GA) and particle swarm optimization (PSO). The findings demonstrate that the GHSA-FTS-LSSVM model provides more accurate predictions than the other tested methods.

So, after reviewing all the above studies, it is possible to highlight all the advantages and disadvantages. Among the advantages, the following can be highlighted: a high percentage of accuracy of forecasting and varied range of forecasting applications. Among the limitations, it is possible to single out the difficulty with the accurate modeling of epidemic processes that requires considering different factors, the incorporation of which complicates forecasting models and makes them less practical. Additionally, the unique transmission dynamics of different diseases and the variability of conditions across locations necessitate that models be rebuilt for each disease and territory. As diseases mutate, quickly adapting models becomes challenging, making long-term predictions difficult; thus, reliable forecasts can typically only be achieved for short-term periods.

3. Materials and Methods

This section is divided into three parts. Section 3.1 presents an overview of neural network architectures for forecasting that were chosen for this study. Section 3.2 presents an overview of the data collected for this study as well as steps taken for its normalization. Section 3.3 presents the methodology that was followed for the development of the time series forecasting models which were applied to the collected data.

3.1. Neural Network Architectures for Forecasting

Presently, numerous neural network (NN) architectures exist, each designed to address a wide array of tasks [53–57]. However, significant variations among these architectures arise in terms of learning speed, execution efficiency, adaptability to diverse platforms, and performance on less capable hardware. Consequently, developers must thoroughly analyze the intricacies of each architecture to identify the most suitable option for their specific task requirements [47–49]. During the study, the following neural network architectures were chosen for forecasting and analysis of time series: N-BEATS, N-HiTS, TCN, RNN, Block RNN, and Transformer Model [44,45,53,56–71].

Architectural design approach for the N-BEATS neural network is guided by several fundamental principles: the foundational architecture is simple and generic, yet capable of deep expression; it avoids dependence on time series-specific feature engineering or input scaling, and lastly, to facilitate interpretability, the architecture is adaptable to enhance the human readability of its outputs [44,46,58].

The basic building block of N-BEATS features a fork architecture. Each block takes an input and produces two output vectors. The first block's input is a history lookback window of varying lengths, typically between 2H and 7H, based on the forecast horizon. Subsequent blocks use residual outputs from the previous blocks as their inputs, generating a forward forecast and a backcast of the input. Internally, each block includes a fully connected network for generating forecasts and backcasts, along with layers that project expansion coefficients onto a set of basis functions to produce the final outputs [44,47,59].

Rather than adding extra connections from the output of each stack to the input of all subsequent stacks—an approach that enhances the trainability of deep architectures but complicates interpretability—N-BEATS employs hierarchical doubly residual topology. This innovative architecture features two residual branches: one that operates on the backcast predictions of each layer and another that runs over the forecast branch of each layer [44,49,58–60]. Figure 1 shows N-BEATS model architecture.

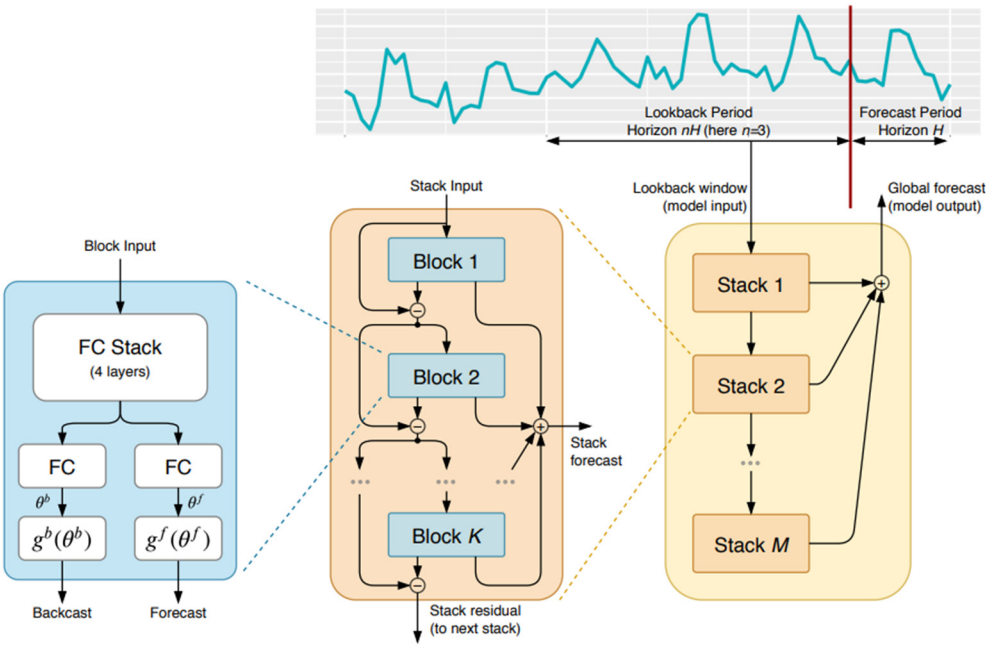

Figure 1. N-BEATS architecture.

N-BEATS also implements ensembling as a more effective regularization technique than alternatives like dropout or L2-norm penalties; although those methods improve individual models, they detract from the ensemble's performance. The effectiveness of

an ensemble relies on diversity, which was achieved through various approaches. To test the performance of N-BEATS architecture, models were trained on three different metrics—sMAPE (symmetric mean absolute percentage error), MASE (mean absolute scaled error), and MAPE (mean absolute percentage error)—and each model was developed using input windows of different lengths for a multi-scale perspective. Additionally, a bagging procedure was performed by incorporating models with different random initializations, resulting in a total of 180 models, with the median used as the aggregation function for the ensemble [44,50,58–60].

With these approaches, the N-BEATS model outperformed pure ML, Statistical, ProLogistica, ML/TS combination, DL/TS hybrid architectures [44,51,58].

N-HiTS reimagines the existing fully connected N-BEATS architecture by improving its input decomposition through multi-rate data sampling and enhancing its output synthesizer with multi-scale interpolation. Extensive experiments demonstrate the significance of these novel architectural components, showing notable improvements in both accuracy and computational efficiency. Multi-rate data sampling of this architecture was achieved by introducing subsampling layers before the fully connected blocks, which greatly reduce memory usage and computational requirements while preserving the ability to model long-range dependencies. Smoothness in multi-step predictions was ensured by lowering the dimensionality of the neural network's outputs and aligning its time scale with that of the final output through multi-scale hierarchical interpolation. This innovative technique can be applied to various architectures beyond the N-HiTS model [45,46].

This architecture also presents a novel approach to synchronizing the input sampling rate with the output interpolation scale across blocks, allowing each block to focus on forecasting its specific frequency band within the time series. N-HiTS achieves leading results on six large-scale benchmark datasets relevant to long-horizon forecasting, including electricity transformer temperature, exchange rates, electricity consumption, highway traffic in the San Francisco Bay Area, weather data, and influenza-like illness [45,46,64].

Like N-BEATS, N-HiTS performs local nonlinear projections onto basis functions across multiple blocks. Each block is made up of MLP that learns to generate coefficients for both the backcast and forecast outputs associated with its basis. The backcast output helps refine the inputs for the subsequent blocks, while the forecasts are aggregated to create the final prediction. The blocks are organized into stacks, with each stack focusing on learning different characteristics of the data through distinct sets of basis functions. N-HiTS consists of S stacks, each containing B blocks, where each block includes an MLP that predicts forward and backward basis coefficients [45,47,64].

N-HiTS, operating in the univariate regime and accepting only the predicted time series' history, significantly outperforms all previous Transformer-based multivariate models using an order of magnitude-less computation [45,52,64]. Figure 2 shows N-HiTS model architecture.

Unlike RNNs, where predictions for later time steps depend on the completion of earlier ones, TCNs leverage convolutions that can be executed in parallel. This allows TCNs to process long input sequences as a whole during both training and evaluation, rather than sequentially as in RNNs [65–69]. TCNs can also adjust their receptive field size through various means, such as stacking additional dilated (causal) convolutional layers, employing larger dilation factors, or increasing filter sizes. This flexibility provides better control over the model's memory requirements and facilitates adaptation to different domains. TCNs have a backpropagation pathway that is independent of the temporal direction of the sequence, thereby mitigating the issues of exploding and vanishing gradients that are prevalent in RNN architectures [56,57,68,69]. This characteristic addresses a significant challenge that has historically necessitated the development of LSTM networks [72–74],

Gated Recurrent Units (GRUs) [56,68], and other architectures. Particularly with long input sequences, LSTMs and GRUs can consume substantial memory to maintain partial results across their multiple cell gates. In contrast, TCNs utilize shared filters across layers, leading to backpropagation paths that depend solely on the network depth, resulting in TCNs typically requiring less memory compared to gated RNNs. Similar to RNNs, TCNs can handle inputs of arbitrary lengths by employing 1D convolutional kernels, making them suitable drop-in replacements for RNNs when processing sequential data of varying lengths [49,75]. Figure 3 shows TCN model architecture.

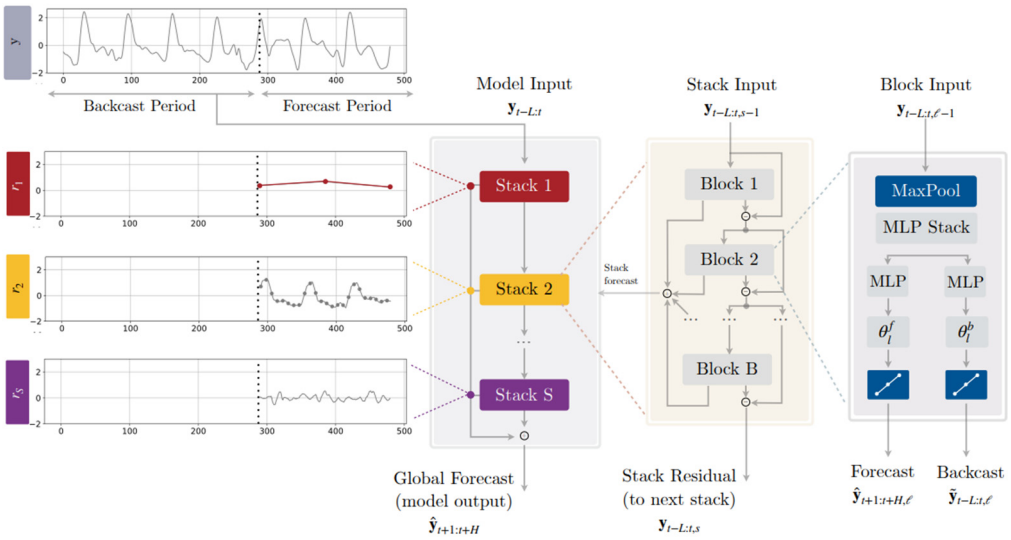

Figure 2. N-HiTS architecture.

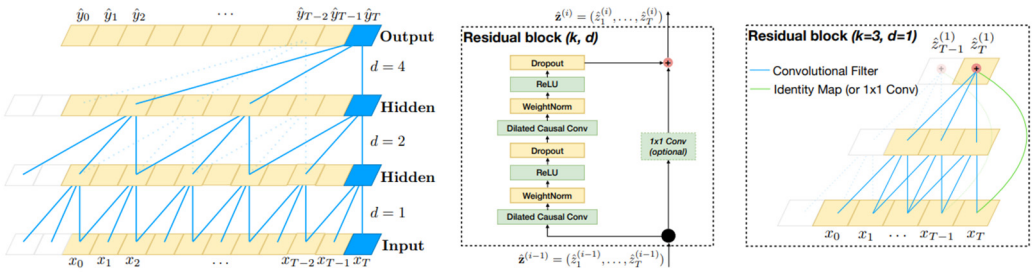

Figure 3. TCN architecture.

However, in evaluation or testing phases, RNNs maintain only a hidden state and the current input to generate predictions, effectively summarizing the entire history with a fixed-length set of vectors, which allows the actual observed sequence to be discarded. Conversely, TCNs must retain the raw sequence up to the effective history length, potentially leading to increased memory requirements during evaluation. Moreover, different domains may necessitate varying amounts of historical context for accurate predictions. Consequently, when transferring a model from a domain with minimal memory needs to one that requires extensive memory, TCNs may underperform due to their insufficient receptive field size [50,75].

DeepAR RNN architecture was designed for probabilistic forecasting, which includes a negative binomial likelihood for count data and special handling for cases where the time series magnitudes vary significantly. This model delivers accurate probabilistic forecasts across various input characteristics, highlighting the effectiveness of modern deep learning approaches in addressing the probabilistic forecasting problem. In addition to achieving better forecast accuracy than past methods, the DeepAR approach offers several key advantages over classical and other global methods: as the model learns seasonal patterns and

dependencies on specific covariates across time series, minimal manual feature engineering is required to capture complex, group-dependent behaviors; DeepAR generates probabilistic forecasts as Monte Carlo samples, enabling consistent quantile estimates for all sub-ranges within the prediction horizon [46,76]. Figure 4 shows RNN model architecture.

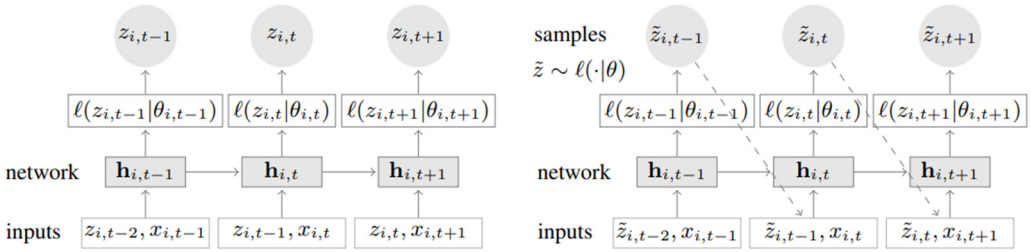

Figure 4. RNN architecture.

Block RNN is a neural network model that uses an RNN encoder to encode fixed-length input chunks and a fully connected network to generate fixed-length output data. This model supports past covariates [68,69].

Transformer Model is a cutting-edge deep learning model introduced in 2017. It utilizes an encoder–decoder architecture, with its key feature being the "multi-head attention" mechanism. This mechanism effectively captures intra-dependencies within both the input and output vectors through "self-attention," as well as inter-dependencies between the input and output vectors through "encoder–decoder attention." The multi-head attention mechanism allows for high parallelization, making the Transformer architecture particularly well-suited for training on GPUs [70,71,77–79].

Figure 5 shows Transformer Model architecture.

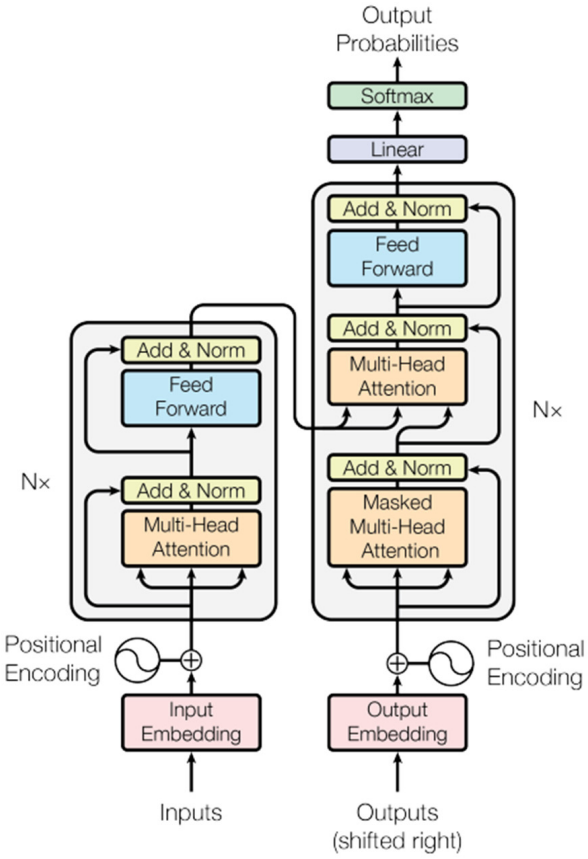

Figure 5. Transformer Model architecture.

3.2. Data Collection

In the course of the study, a systematic collection of data on the spread of infectious diseases in Ukraine was carried out from December 2016 to January 2024. Monthly reports were obtained from national healthcare databases, namely the Public Health Center of the Ministry of Health of Ukraine. The data collected by the Public Health Center are provided in accordance with reporting form No. 1 [80]; the reports give absolute figures and intensive indicators per 100,000 population. The data is given in a comparison for a certain period of time for the current and previous years, as well as for a full year (12 months). To take into account fluctuations in the number of the population during the studied period, the data were normalized according to the estimates of the number of the population of the State Statistics Service of Ukraine. The absolute values were normalized to reflect the number of diseases for the current month per 1,000,000 population of Ukraine for the current year. The following formula was used to normalize the number of patients:

$$\frac{abs.\ number\ of\ cases\ per\ month\ \times\ 1,000,000}{population\ per\ year} \quad (1)$$

This normalization allowed analysis per 1,000,000 population, facilitating comparisons across months and years. In cases where there were duplicate reports or conflicting data, a consensus approach was used, prioritizing the months with the highest number of reported cases to ensure the accuracy and reliability of the data set. This thorough data processing was essential to ensure a clear and accurate representation of infectious disease trends in Ukraine during the specified time period. Due to some unreliable data present in the original dataset (latter reports include diseases that were not present in the former reports as well as some inconsistencies in the number of cases in former reports) among 65 infectious diseases, 57 were chosen, including Cholera, Typhoid, Paratyphoid A, B, C and others. These diseases were manually reviewed for the highest quality training data.

Each infectious disease was modeled as a separate univariate time series, and no aggregation across different diseases was performed. In the global learning setup, models were trained jointly on a collection of parallel disease-specific time series, where the same model parameters were shared across all series, but the temporal sequences remained independent. Diseases were not grouped into epidemiological transmission categories (e.g., respiratory, water-borne, vector-borne, and so on).

The monthly national surveillance reports did not contain explicit missing months for the diseases included in the final dataset. However, inconsistencies across successive reports were observed, including retrospective corrections and occasional reclassification of cases. To ensure consistency, a manual curation step was applied, during which diseases with unstable or incomplete reporting histories were excluded entirely from further analysis, resulting in the final set of 57 diseases.

For the retained diseases, no temporal interpolation, smoothing, or artificial gap filling was applied, in order to avoid introducing synthetic temporal structures into outbreak dynamics. Zero values, when present, were kept unchanged, as they may reflect either true absence of reported cases or disruptions in case registration during crisis periods.

Graphs of diseases with normalized values were constructed and analyzed. Figure 6 shows graphs of the cases of infectious diseases in the time span from December 2016 to January 2024.

Among 57 selected infectious diseases 22 were observed to have increased in the number of cases after the beginning of war in Ukraine (24 February 2022), such as giardiasis cases with the average before the war of 4.53 increased to 10.06, which is a 121.91% increase, intestinal protozoan diseases with the average before the war of 5.06 increased to 11.19, which is a 120.9% increase.

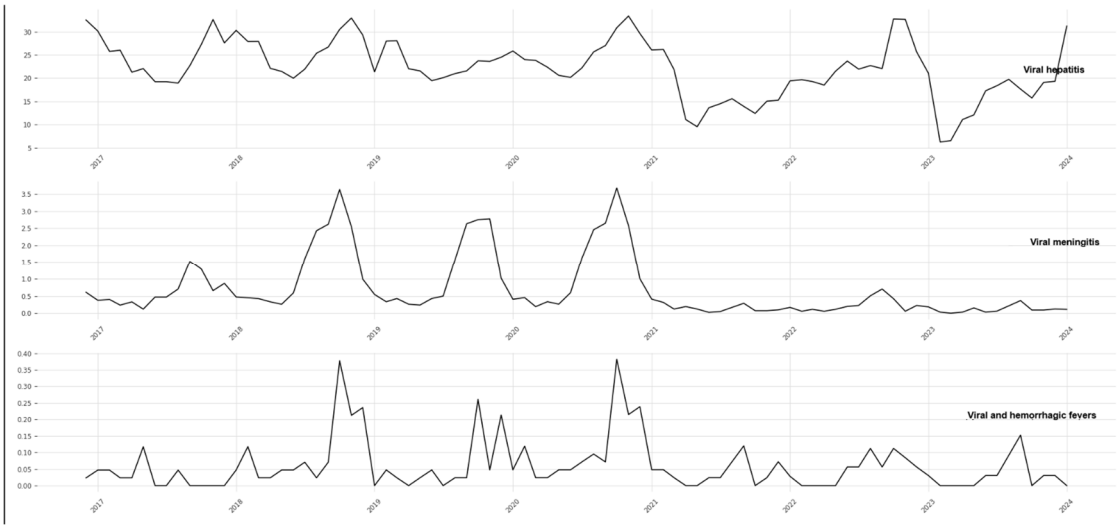

Figure 6. Graphs of the cases of infectious diseases.

Overall, 35 infectious diseases were observed to have a decrease in number of cases, with an average of 35.52% decrease in the number of cases, and 22 diseases with an average of 62.38% increase in the number of cases.

With these numbers, the impact of the emergency situations is obvious. Russia's large-scale aggression in Ukraine has led to a significant emergency situation that has impacted all facets of life and triggered additional emergencies, such as floods and droughts resulting from the damage to the Kakhovskaya Hydroelectric Power Plant. Other risks include potential radionuclide contamination from incidents at the Chernobyl and Zaporizhzhya Nuclear Power Plants, forest fires on the Kinburn spit that have devastated over 1500 hectares of forest, and chemical substance emissions, including chlorine and ammonia. In the context of these emergencies, the dynamics and manifestations of infectious disease epidemics may differ from their natural progression. Key risk factors influencing the epidemic situation amid the cascade of emergencies instigated by the war include significant population migration, overcrowding in bomb shelters and migration routes, heightened stress levels leading to increased vulnerability to infections, disruption of water and energy supplies, a surge in rodent populations and related epizootics, food contamination, runoff of various chemicals into water bodies, flooding of natural ecosystems, activation of transmission mechanisms for infectious agents, a rise in stray animals and their interactions with wildlife, and contamination of areas due to rocket and artillery strikes and landmines [81,82].

3.3. Methodology for Performing Time Series Forecasting

A normalized dataset of infectious disease cases in Ukraine for the period from December 2016 to January 2024 served as the basis for training several advanced neural network architectures. These data were also normalized between 0 and 1 to improve neural network training. The models used in this study included RNNs, Block RNNs, N-BEATS, TCNs, Transformer Models, and N-HiTS.

Each neural network was trained in two separate approaches: first, using all time series covering all infectious diseases present in the dataset; and second, focusing on a single time series for a specific infectious disease. A single neural network model was trained jointly on the entire collection of disease-specific time series. Each disease constituted an independent univariate sequence, while the model parameters were shared across all series. During training, loss was computed across all series and time windows, enabling the model to learn common temporal structures across different infections without aggregating case counts. We wanted to not only find the best neural network architecture for our task,

but find the best way to train it. Training an independent model for each infection is appropriate since independent models allow each estimator to specialize in the temporal dynamics unique to its respective infection without interference from dissimilar infections. Training global (or pooled) models using the full dataset covering all infectious diseases can help uncover if infections share common drivers and allow the models to learn generalizable temporal structures. This approach is preferable since a single model simplifies deployment and maintenance. Larger aggregated datasets reduce variance and improve generalization [83–85].

The neural networks were created in Python 3.12.12 using Darts library in Google Colab [86–88]. Darts is a Python library designed for intuitive forecasting and anomaly detection in time series data. It features a range of models, from traditional ones like ARIMA [89–92] to advanced deep neural networks. All forecasting models can be utilized similarly, with fit() and predict() functions, akin to scikit-learn. The library simplifies backtesting, allows for the combination of predictions from different models, and incorporates external data. Darts accommodates both univariate and multivariate time series and models. The machine learning-based models can be trained on large datasets with multiple time series, and several models provide robust support for probabilistic forecasting [93].

The RNN model was created with the size for feature maps for each hidden RNN layer of 25 and 1 recurrent layer [94–106].

The Block RNN model was created with a size of 25 feature maps for each hidden RNN layer and 1 layer in the RNN module and ReLU activation function that is applied between the layers of the fully connected network.

The N-BEATS model was created with 30 stacks and 1 block for each stack, as well as 4 fully connected layers preceding the final forking layers in each block of every stack. Each block of every stack had 256 neurons that make up each fully connected layer. The dimensionality of the waveform generator parameters, also known as expansion coefficients, had the value of 5 with the degree of the polynomial used as waveform generator in trend stacks of 2 with ReLU activation function of encoder/decoder intermediate layer.

The N-HiTS model was created with 3 stacks and 1 block per stack with 512 neurons that make up each fully connected layer in each block of every stack and 2 fully connected layers preceding the final forking layers in each block of every stack. The dropout probability used in fully connected layers had the value of 0.1 with ReLU activation function.

The TCN model was created with the size of every kernel in a convolutional layer of 3 and 3 filters in a convolutional layer. The base of the exponent that determines the dilation on every level had the value of 2 and the dropout rate of 0.2.

The Transformer Model was created with 64 expected features in the transformer encoder/decoder inputs, 4 heads in the multi-head attention mechanism and 3 encoder/decoder layers in the encoder/decoder. The dimension of the feedforward network model had the value of 512 with ReLU activation function.

For both training configurations, the models used historical data from the previous 24 months to predict cases for the next 6 months. These time frames were intended to capture trends and patterns that could improve forecasting accuracy. Figure 7 shows training results of neural network architectures on all time series in the following order: N-HiTS, N-BEATS, Block RNN, RNN, TCN, Transformer. Models were trained in Google Colab using the T4 GPU hardware accelerator. N-BEATS training took the least amount of time, which was approximately 1 h and 10 min, while Transformer took the most amount of time, training of which took around 2 h.

Figure 8 shows training results of neural network architectures on a single time series at a time in the following order: N-HiTS, N-BEATS, Block RNN, RNN, TCN, Transformer.

RNN training took the least amount of time, which was approximately 17 min, while Transformer took the most amount of time, training of which took around 30 min.

Figure 7. Training of neural network architectures on all time series.

Figure 8. Training of neural network architectures on a single time series.

The MAPE, also known as the mean absolute percentage deviation (MAPD), was used to determine the forecasting results [107]. It is worth noting that most infectious diseases do not have some seasonal fluctuations or trends, which is reflected in the predictions of neural networks. Neural networks gave better predictions on time series that fluctuate relatively constantly (for example, the number of diseases increases in summer and decreases in winter). Figure 9 shows neural network predictions on time series with clear seasonality.

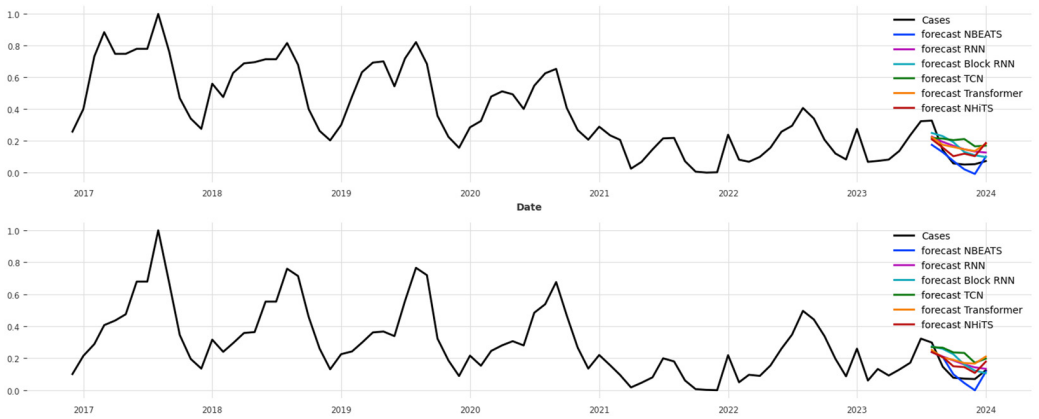

Figure 9. Neural networks predictions on time series with clear seasonality.

Figure 10 shows the prediction of neural networks on time series with no clear seasonality.

Figure 10. Neural network predictions on time series with no clear seasonality.

Neural networks designed for forecasting tend to perform better on datasets with visible fluctuations and/or trends, such as seasonal patterns. When fluctuations, such as seasonal rises and drops, are clearly visible, the network can recognize these patterns and incorporate them into its predictions. In datasets with pronounced seasonal effects or trends, the network can discover features that capture these fluctuations, improving forecasting accuracy. Datasets with clear seasonal effects and trends provide temporal dependencies that neural networks can exploit to make more informed predictions.

4. Results

To analyze the prediction accuracy of neural networks, a 95% confidence interval was used [108]. Thus, the mean MAPE prediction values of neural networks trained using all time series covering all infectious diseases 95% of the time are shown in Table 1.

Table 1. Predictions of neural network architectures that were trained on all time series.

Neural Network	Average MAPE, %	Average MAE	Average RMSE
TCN	110.91	1480.7	1780.4
Block RNN	76.79	1214.9	1520.1
N-HiTS	75.31	1165.7	1454.3
RNN	71.35	1184.5	1490.3
Transformer	67.99	1304.9	1406.0
N-BEATS	63.56	1140.8	1322.6

The better results of N-BEATS can be attributed to its residual block architecture and explicit signal decomposition strategy, which are suited to epidemiological time series characterized by strong seasonal patterns, long-term trends, and so on. By iteratively modeling and subtracting trend- and seasonality-related components, N-BEATS can progressively refine residual dynamics, which is particularly beneficial in noisy data affected by reporting delays and crisis-driven disruptions. In contrast, recurrent and convolutional models tend to accumulate errors over long horizons and are more sensitive to non-stationary shifts in baseline incidence levels.

The average prediction MAPE values of neural networks trained to focus on one time series for a specific infectious disease 95% of the time are shown in Table 2.

Table 2. Predictions of neural network architectures that were trained on a single time.

Neural Network	Average MAPE, %	Average MAE	Average RMSE
TCN	160.02	1435.7	1753.2
Block RNN	149.43	1320.2	1626.2
N-HiTS	98.36	1466.3	1892.5
RNN	153.06	1307.3	1619.6
Transformer	122.72	1452.6	1764.2
N-BEATS	82.92	1330.3	1660.0

Notably, neural networks trained on multiple time series showed better performance compared to those trained on single time series. This improvement can be attributed to the ability of the models to use common information about different diseases, which enriched their learning process and contributed to more reliable predictions. The results highlight the potential of multi-time series approaches to improve the accuracy of neural network-based infectious disease forecasting. This discovery suggests that infectious diseases can influence each other and their spread, indicating a complex interaction between different pathogens.

RNNs and Block RNNs rely on sequential processing, which often struggles with long-range dependencies, vanishing gradients, and noise accumulation—common problems

in epidemic data that include sudden surges, reporting delays, and irregular patterns. N-BEATS uses a deep fully connected architecture, enabling stable optimization and fast training without the memory bottlenecks of recurrent models.

N-BEATS uses posteriori interpretable blocks (trend and seasonality) that align well with real epidemic patterns such as monthly reporting cycles, gradual waves, and long-term drifts. This gives it an advantage over Transformers, which lack built-in time series structure and depend heavily on positional encodings.

5. Discussions

The findings of this study demonstrate a substantial change in infectious disease incidence in Ukraine during the examined period. Using monthly surveillance reports from December 2016 to January 2024, we constructed a normalized dataset per 1,000,000 population and selected 57 diseases after resolving inconsistencies and duplicate records through a consensus procedure. After 24 February 2022, 22 of 57 monitored diseases increased, with an average increase of 62.38%, while 35 diseases decreased with an average decrease of 35.52%. These shifts are compatible with prior evidence that conflict and cascading emergencies can elevate infectious disease risks through population displacement, overcrowding, disruption of healthcare access, and damage to water and sanitation systems [109]. At the same time, the observed direction of change in routine surveillance data should be interpreted as a combined signal of transmission dynamics and the stability of case detection and reporting. In war conditions, delayed reporting, reduced access to diagnostics, and disrupted notification pathways can lead to underestimation of observed counts, even when the true incidence does not decrease. Evidence from Ukraine suggests that formal infectious disease surveillance was disrupted following the 2022 invasion, and that open-source epidemic intelligence was used to some extent to compensate for the reduced visibility into outbreaks [110].

The normalization of absolute monthly counts by annual population estimates improved comparability across months and years. However, it also introduces additional uncertainty when population size changes rapidly due to displacement and migration. In such settings, denominator uncertainty can influence estimated rates, particularly for diseases with relatively low incidence. A practical implication is that sensitivity analyses with alternative denominator scenarios, as well as stratified analyses where regional data are available, would strengthen the interpretation of temporal changes and support more targeted public health conclusions.

In parallel with the epidemiological observations, this study evaluated several neural network architectures for forecasting trends in infectious diseases. Models used historical data from the previous 24 months to predict cases for the next 6 months, reflecting a multi-horizon forecasting setup that is challenging for monthly surveillance series. Consistent with earlier studies in time series forecasting, the N-BEATS architecture provided the best overall performance among the tested models and exhibited efficient training dynamics [111]. N BEATS is a deep residual architecture designed for forecasting that can learn components resembling trend and seasonality, which can be advantageous when reporting cycles, and gradual epidemic waves create structured temporal dependencies.

Models trained on multiple time series outperformed those trained on a single disease time series, supporting the hypothesis that shared structure across diseases can be leveraged to improve stability and generalizability. This result aligns with the broader literature on global forecasting, where training on multiple related series provides an implicit form of multi-task learning and regularization, thereby improving performance under noisy and incomplete data [76]. However, cross-series learning can also introduce negative transfer when diseases differ substantially in transmission route, intervention sensitivity, or surveil-

lance intensity. This motivates structured pooling strategies such as grouping diseases by transmission mechanism or fitting shared representations with disease-specific output heads, which would preserve the benefits of global learning while reducing inappropriate parameter sharing.

Latent representation learning, inter-disease dependence, and attention-based temporal model global training setup shares parameters across multiple disease-specific series; it does not explicitly extract shared latent drivers or model inter-disease dependence. A relevant methodological line of work treats large collections of related time series as being generated by a low-dimensional set of global latent factors combined with series-specific temporal dynamics. For example, Deep Factors learns global latent factors that capture shared structure across many series while retaining local dynamics for each series, providing a scalable mechanism for representing common hidden drivers beyond simple parameter sharing [112]. When dependencies between series are meaningful and can be represented explicitly, graph-based extensions incorporate a learned or predefined graph to model correlated behavior among series in a principled probabilistic framework [113]. In the context of infectious disease surveillance, such approaches are directly relevant because they offer a pathway to represent shared seasonal and reporting effects, as well as cross-disease coupling or co-movement, in an explicit latent space rather than relying on implicit regularization from pooled training alone.

In addition, the manuscript currently reports results from a baseline Transformer, but attention-based forecasting has advanced substantially beyond vanilla self-attention. The Temporal Fusion Transformer is a widely used attention-based architecture for multi-horizon forecasting that combines recurrent processing for local patterns with interpretable self-attention for long-range dependencies and is especially suitable when heterogeneous covariates are available [114]. For long-horizon settings, subsequent Transformer-family models have proposed mechanisms that improve efficiency or inductive bias for temporal structure, including long-sequence attention approximations (e.g., Informer [115]) and decomposition-based Transformer forecasters tailored to long-term series forecasting (e.g., Autoformer [116]; FEDformer [117]). These strands of work collectively motivate attention-based and representation-based directions as substantive extensions to our current benchmark.

The present study did not include a dedicated analysis of the contribution of individual input features and temporal lags to the generated forecasts. The models were considered as end-to-end forecasting systems, and the internal representations learned by the neural networks were not examined in terms of which specific parts of the historical window or potential exogenous factors had the strongest influence on the results.

Forecast accuracy varied across diseases, with models performing better for time series exhibiting clear seasonal fluctuations or visible trends. This observation is expected because seasonal structure provides recurrent patterns that neural forecasters can exploit. In contrast, diseases with irregular outbreaks, low counts, or abrupt regime shifts present a limited repeatable signal in the autoregressive history alone. This limitation is likely amplified by the war period, which introduces distribution shifts and structural breaks in both transmission and surveillance processes. In such contexts, purely endogenous forecasting can be insufficient, and performance improvements may require incorporating external signals that reflect underlying drivers of transmission and detection.

The study identifies key limitations and outlines directions for future research. The restricted spatial and temporal scope, reliance on routine surveillance data, and sensitivity to sudden shifts constrain generalizability. Future improvements are likely to come from incorporating exogenous factors such as weather conditions, mobility measures, and vaccination activity, which can shape real-world transmission but were not included in the current

models. Architectures designed to integrate heterogeneous covariates in multi-horizon settings, such as the Temporal Fusion Transformer, provide a natural technical pathway for this extension [114]. In addition, because reporting delays and backfill can distort the most recent observations in surveillance systems, integrating nowcasting methods that explicitly adjust for delays can improve both training targets and near-term forecasting accuracy [118]. These extensions would better align deep forecasting with the biological, social, and operational determinants of infectious disease patterns in emergency contexts.

6. Conclusions

The collected and normalized data of infectious diseases showed an average of 62.38% increase in the number of cases for 22 out of 57 diseases. This data shows a negative impact of emergency situations on the population of Ukraine in the scope of healthcare and well-being.

The developed neural networks were trained and had their performance compared. N-BEATS model outperformed the other neural network models with 63.56% average MAPE. Although N-BEATS does not provide explicit epidemiological explanations, its internal decomposition into trend- and seasonality-related components allows partial qualitative interpretation of forecast drivers. In practice, this makes it possible to distinguish whether predictions are dominated by baseline seasonal cycles or by longer-term shifts in incidence levels, which may support short-term monitoring and operational decision-making, even when transmission mechanisms are not explicitly modeled. Neural networks trained on multiple time series outperformed those trained on single time series.

The key technologies used in the system are RNNs, Block RNNs, N-BEATS, TCNs, Transformer Model, and N-HiTS, libraries for developing a neural network and its training, including Tensorflow and Darts.

For testing, a separate independent dataset was collected that was not part of the dataset for training. After that, the neural networks were tested and their accuracy was determined. It is important to acknowledge that they were trained exclusively on data from a single country and over a limited period (2016–2024). This constrained spatial and temporal scope may limit the models' ability to generalize to other regions, different epidemiological contexts, or newly emerging diseases. The reported performance should not be interpreted as universally applicable across different healthcare systems or surveillance infrastructures, and external validation on independent multi-country datasets is required before operational deployment. Another limitation of this study is the lack of explicit epidemiological stratification of diseases by transmission mechanisms or clinical categories (e.g., respiratory, water-borne, or vector-borne). The model evaluation in this study was based solely on point forecasts and deterministic accuracy metrics, without explicit estimation of predictive uncertainty or confidence intervals. This design choice was aligned with the study objective of benchmarking neural architectures and training strategies under a uniform evaluation protocol, where deterministic metrics allowed a transparent comparison of relative model performance. The study focuses on comparing the point-forecasting accuracy of neural network architectures rather than on probabilistic forecasting for decision support. Point forecasts enable a clear and consistent evaluation of predictive performance across models without introducing additional methodological variability associated with uncertainty quantification techniques. While uncertainty estimates are important for public health applications, they fall outside the scope of this comparative analysis and are left for future works. Incorporating probabilistic forecasting frameworks, ensemble-based uncertainty estimation, or stochastic regularization techniques such as Monte Carlo dropout will be an important direction for future research.

The study did not estimate the contribution of individual input lags or potential exogenous variables to the generated forecasts, and the learned temporal representations were not examined to identify dominant predictive drivers. Incorporating feature-importance assessment and sensitivity analysis would enhance transparency and help link predictions to plausible epidemiological mechanisms, thereby increasing the practical value of the forecasting framework.

Future work should therefore evaluate the models using more diverse, multi-regional datasets and extended time horizons to strengthen their robustness and broader applicability.

Neural networks can be an integral part for the forecasting of the spread of infectious diseases. However, without a clear seasonality in the data for some infectious diseases, all of the studied neural network architectures showed mediocre performance. Infectious disease transmission involves complex interactions between various factors, including host behavior, environmental conditions, and pathogen characteristics. Capturing these dynamics accurately in a model can be difficult.

In future work, the forecasts could benefit from bringing in additional exogenous factors, such as weather conditions, mobility data, or vaccination activity, which often shape real-world transmission but were not included in our current models. Future research should also incorporate latent representation learning and dimensionality reduction techniques to explicitly model shared hidden drivers and correlations among multiple diseases. These external signals may help reduce some of the limitations that were encountered—particularly the models' sensitivity to sudden shifts in case patterns and their difficulty capturing periods of low incidence. The study was also constrained by the availability and quality of surveillance data, which limited both the temporal resolution and the ability to compare model behavior across different regions. Expanding the dataset and testing the models in more varied settings would allow for a clearer understanding of how biological and environmental drivers influence performance. Taken together, these directions could help make future versions of the forecasting framework more reliable and better aligned with the underlying biology of disease spread.

Author Contributions: Conceptualization, O.K. and D.C.; methodology, O.K., Y.K. and I.S.; software, O.K.; validation, Y.K., D.C. and G.K.; formal analysis, I.S. and G.K.; investigation, D.C., Y.K. and O.K.; resources, O.K., G.K. and D.C.; data curation, Y.K. and I.S.; writing—original draft preparation, O.K. and I.S.; writing—review and editing, Y.K. and D.C.; visualization, O.K. and G.K.; supervision, Y.K. and I.S.; project administration, Y.K., I.S. and D.C.; funding acquisition, D.C. All authors have read and agreed to the published version of the manuscript.

Funding: The study was funded by the National Research Foundation of Ukraine in the framework of the research project 2023.03/0197 on the topic "Multidisciplinary study of the impact of emergency situations on the infectious diseases spreading to support management decision-making in the field of population biosafety".

Data Availability Statement: The original contributions presented in this study are included in the article. Further inquiries can be directed to the corresponding author.

Conflicts of Interest: The authors declare no conflicts of interest.

Abbreviations

The following abbreviations are used in this manuscript:

N-BEATS	Neural Basis Expansion Analysis for Time Series Forecasting
N-HiTS	Neural Hierarchical Interpolation for Time Series Forecasting
TCN	Temporal Convolutional Network
RNN	Recurrent Neural Network
GBM	Gradient Boosting Machine

kNN	K-Nearest Neighbor
EnKF	Ensemble Kalman Filter
LSTM	Long Short-Term Memory
MLP	Multilayer Perceptron
GHSA	Global Harmony Search Algorithm
FTS	Fuzzy Time Series
LSSVM	Least Squares Support Vector Machines
FCS	Fuzzy C-Means Clustering
ARIMA	Autoregressive Integrated Moving Average
GA	Genetic Algorithm
PSO	Particle Swarm Optimization
NN	Neural Network
sMAPE	Symmetric Mean Absolute Percentage Error
MASE	Mean Absolute Scaled Error
MAPE	Mean Absolute Percentage Error
GRU	Gated Recurrent Units

References

1. Goniewicz, K.; Burkle, F.M.; Horne, S.; Borowska-Stefańska, M.; Wiśniewski, S.; Khorram-Manesh, A. The Influence of War and Conflict on Infectious Disease: A Rapid Review of Historical Lessons We Have Yet to Learn. *Sustainability* **2021**, *13*, 10783. [CrossRef]
2. Pennington, H. The Impact of Infectious Disease in War Time: A Look Back at WW1. *Future Microbiol.* **2019**, *14*, 165–168. [CrossRef]
3. Diseases, T.L.I. War and Infectious Diseases: Brothers in Arms. *Lancet Infect. Dis.* **2022**, *22*, 563. [CrossRef]
4. Ergönül, Ö.; Tülek, N.; Kayı, I.; Irmak, H.; Erdem, O.; Dara, M. Profiling Infectious Diseases in Turkey after the Influx of 3.5 Million Syrian Refugees. *Clin. Microbiol. Infect.* **2019**, *26*, 307–312. [CrossRef]
5. Daw, M.A. The Impact of Armed Conflict on the Epidemiological Situation of COVID-19 in Libya, Syria and Yemen. *Front. Public Health* **2021**, *9*, 667364. [CrossRef] [PubMed]
6. Muhjazi, G.; Gabrielli, A.F.; Ruiz-Postigo, J.A.; Atta, H.; Osman, M.; Bashour, H.; Al Tawil, A.; Husseiny, H.; Allahham, R.; Allan, R. Cutaneous Leishmaniasis in Syria: A Review of Available Data during the War Years: 2011–2018. *PLoS Negl. Trop. Dis.* **2019**, *13*, e0007827. [CrossRef]
7. Ottolini, M.; Cirks, B.; Madden, K.B.; Rajnik, M. Pediatric Infectious Diseases Encountered During Wartime—Part 1: Experiences and Lessons Learned From Armed Conflict in the Modern Era. *Curr. Infect. Dis. Rep.* **2021**, *23*, 27. [CrossRef] [PubMed]
8. Ngo, N.V.; Pemunta, N.V.; Muluh, N.E.; Adedze, M.; Basil, N.; Agwale, S. Armed Conflict, a Neglected Determinant of Childhood Vaccination: Some Children Are Left Behind. *Hum. Vaccines Immunother.* **2019**, *16*, 1454–1463. [CrossRef] [PubMed]
9. Papageorgiou, V.E. Boosting epidemic forecasting performance with enhanced RNN-type models. *Oper. Res. Int. J.* **2025**, *25*, 77. [CrossRef]
10. Ramani, R.; Ganesh, S.S.; Rao, S.P.V.S.; Aggarwal, N. Integrated Multi-Modal 3D-CNN and RNN Approach with Transfer Learning for Early Detection of Alzheimer's Disease. *Iran J. Sci. Technol. Trans. Electr. Eng.* **2025**, *49*, 383–407. [CrossRef]
11. Priya, E.K.; Sasikala, S. A novel optimization technique using deep learning approach for prediction of multiple sclerosis by implementing the architect of Hybrid—RNN & LSTM. *Soft Comput.* **2025**, *29*, 6321–6331. [CrossRef]
12. Afify, H.; Mohammed, K.; Hassanien, A. Leveraging hybrid 1D-CNN and RNN approach for classification of brain cancer gene expression. *Complex Intell. Syst.* **2024**, *10*, 7605–7617. [CrossRef]
13. Veena, H.N.; Patil, K.K.; Vanajakshi, P.; Ambore, A.; Gowda, N.C. An Enhanced RNN-LSTM Model for Fundus Image Classification to Diagnose Glaucoma. *SN Comput. Sci.* **2024**, *5*, 514. [CrossRef]
14. Vincent, A.N.; Sakthidasan, K.; Sunhaloo, M.S.; Clement, J.C.; Laloo, N.; Bagurubumwe, U. Comparative analysis of RNN, LSTM and CNN algorithms for marine data prediction. *J. Coast. Conserv.* **2025**, *29*, 73. [CrossRef]
15. Chen, J.; Zhang, H.; Zou, Q.; Liao, B.; Bi, X.-A. Multi-kernel Learning Fusion Algorithm Based on RNN and GRU for ASD Diagnosis and Pathogenic Brain Region Extraction. *Interdiscip. Sci. Comput. Life Sci.* **2024**, *16*, 755–768. [CrossRef]
16. Jothi, R.; Jayanthi, K. A deep multi-filtering network based on dilated mask RCNN framework with self-attention RNN model for segmenting and classifying bone fracture. *Multimed. Tools Appl.* **2025**, *84*, 29815–29841. [CrossRef]
17. Ji, G.; Liu, P. RNN-Based Multiple Instance Learning for the Classification of Histopathology Whole Slide Images. In *Proceedings of the International Conference on Medical Imaging and Computer-Aided Diagnosis (MICAD 2023)*; Su, R., Zhang, Y.D., Frangi, A.F., Eds.; Lecture Notes in Electrical Engineering; Springer: Singapore, 2024; Volume 1166, pp. 329–339. [CrossRef]

18. Chopra, S.; Agarwal, P.; Ahmed, J.; Biswas, S.S.; Obaid, A.J. RNN-CNN Based Hybrid Deep Learning Model for Mental Healthcare. In *Proceedings of the International Conference on Artificial Intelligence and Its Application. ICAIA 2024; Algorithms for Intelligent Systems*; Yadav, A., Joshi, A.M., Ergezer, M., Balas, V.E., Eds.; Springer: Singapore, 2025; pp. 411–424. [CrossRef]
19. Ning, J.; Zhang, W. Speech-based emotion recognition using a hybrid RNN-CNN network. *Signal Image Video Process.* **2025**, *19*, 124. [CrossRef]
20. Gupta, D.; Kaushal, M.; Sharma, A. Reinforcement Learning Based Video Summarization Using Attention Aware Dilated RNN. *New Gener. Comput.* **2025**, *43*, 19. [CrossRef]
21. Amini, S.S.; Mandala, S.; Pramudyo, M. Myocardial Infarction Prediction Using RNN Deep Learning Algorithm on Phonocardiogram Signals. In Proceedings of the 11th International Conference on Information and Communication Technology (ICoICT), Melaka, Malaysia, 23–24 August 2023. [CrossRef]
22. Gollapalli, V.S.T.; Jadon, R.; Budda, R.; Srinivasan, K.; Chauhan, G.S.; Awotunde, J.B. Adaptive Hellinger Distance CS and GELU-RNN: Advanced Solutions for Feature Optimization and Cloud Threat Detection. *SN Comput. Sci.* **2025**, *6*, 515. [CrossRef]
23. Karamchandani, A.; Mozo, A.; Vakaruk, S.; Gómez-Canaval, S.; Sierra-García, J.E.; Pastor, A. Using N-BEATS ensembles to predict automated guided vehicle deviation. *Appl. Intell.* **2023**, *53*, 26139–26204. [CrossRef]
24. Sbrana, A.; Lima de Castro, P.A. N-BEATS Perceiver: A Novel Approach for Robust Cryptocurrency Portfolio Forecasting. *Comput. Econ.* **2024**, *64*, 1047–1081. [CrossRef]
25. Kahlessenane, Y.; Bouaziz, F.; Siarry, P. ECG Heartbeats Classification Using Two-Dimensional Deep Learning Convolutional Neural Network. *Circuits Syst. Signal Process* **2025**, *44*, 7505–7525. [CrossRef]
26. de Jesus, L.C.; Fernández-Navarro, F.; Carbonero-Ruz, M. Enhancing financial time series forecasting through topological data analysis. *Neural Comput. Appl.* **2025**, *37*, 6527–6545. [CrossRef]
27. Shukla, P.K.; Chakraborty, T.; Sari, M.; Sarout, J.; Mandal, P.P. Salt rock creep deformation forecasting using deep neural networks and analytical models for subsurface energy storage applications. *Sci. Rep.* **2025**, *15*, 34560. [CrossRef]
28. Wu, Z.; Li, F.; Yan, Y.; Zhao, D.; Guo, J. Bridge Monitoring Data Reconstruction Based On N-BEATS-Transformer Model. In Proceedings of the 36th Chinese Control and Decision Conference (CCDC), Xi'an, China, 25–27 May 2024. [CrossRef]
29. Surribas-Sayago, G.; Fernández-Rodríguez, J.D.; Dominguez, E. Advancing Photovoltaic Forecasting with Neural Networks: Integrating N-Beats and Sequential Models with Fourier Analysis. In *Proceedings of the Ibero-American Conference on Artificial Intelligence. IBERAMIA 2024*; Lecture Notes in Computer Science; Correia, L., Rosá, A., Garijo, F., Eds.; Springer: Cham, Switzerland, 2025; Volume 15277, pp. 287–297. [CrossRef]
30. Aiwansedo, K.; Bosche, J.; Badreddine, W.; Kermia, M.H.; Djadane, O. CNN-N-BEATS: Novel Hybrid Model for Time-Series Forecasting. In *Proceedings of the International Conference on Deep Learning Theory and Applications. DeLTA 2024, Dijon, France, 10–11 July 2024*; Communications in Computer and Information Science; Fred, A., Hadjali, A., Gusikhin, O., Sansone, C., Eds.; Springer: Cham, Switzerland, 2024; Volume 2171, pp. 38–57. [CrossRef]
31. Shi, P.; Tang, M.; Wang, Q.; Ma, X. Optimization of TCN-BiLSTM for dissolved oxygen prediction based on improved sparrow search algorithm. *Sci. Rep.* **2025**, *15*, 30790. [CrossRef]
32. Qu, X.; Zhu, J.; Lu, P.; Li, J. TCN-transformer crusher fault prediction model based on data augmentation and dual-stream feature fusion. *J. Mech. Sci. Technol.* **2025**, *39*, 6567–6577. [CrossRef]
33. Wang, W.; Xu, Y.; Liu, Y.; Bai, L.; Li, G.; Jing, X. Short-Term Power Load Forecasting Based on GJO-TCN-BiGRU-TPA. *J. Electr. Eng. Technol.* **2025**, *21*, 251–261. [CrossRef]
34. Ahirwar, M.S.; Soni, V. TCN-BiSRU-V2 fall detection model with performance evaluation and comparative analysis. *Discov. Comput.* **2025**, *28*, 186. [CrossRef]
35. Huang, G.; Zhang, Y.; Wu, T.; Shi, P.; Wan, M. Roll bending forming curvature radius prediction based on the CNN-TCN-TPA neural network model. *Int. J. Mater. Form.* **2025**, *18*, 34. [CrossRef]
36. Yuan, J.; Li, Y. Wastewater quality prediction based on channel attention and TCN-BiGRU model. *Environ. Monit. Assess.* **2025**, *197*, 219. [CrossRef]
37. Wang, J.; Xia, L.; Wen, X. Cmf-transformer: Cross-modal fusion transformer for human action recognition. *Mach. Vis. Appl.* **2024**, *35*, 114. [CrossRef]
38. Lijin, P.; Ullah, M.; Vats, A.; Cheikh, F.A.; Kumar, G.S.; Nair, M.S. PolySegNet: Improving polyp segmentation through swin transformer and vision transformer fusion. *Biomed. Eng. Lett.* **2024**, *14*, 1421–1431. [CrossRef]
39. Dickson, B.; Mochizuki-Freeman, J.; Kabir, R.; Tiganj, Z. Time-Local Transformer. *Comput. Brain Behav.* **2025**. [CrossRef]
40. Deng, X.; Fang, X.; Huang, G.; Fu, J. Efficient vision transformer: Application of data-efficient image transformer for aero engine bearing fault classification. *Signal Image Video Process.* **2025**, *19*, 515. [CrossRef]
41. Liu, Y.; Sun, J.; Dong, W.; Zhang, L.; Wang, C.; Deng, F. Deep Learning-Based Flight Trajectory Prediction Using Time Series Decomposition. In *Proceedings of the International Conference on Guidance, Navigation and Control. ICGNC 2024*; Yan, L., Duan, H., Deng, Y., Eds.; Lecture Notes in Electrical Engineering; Springer: Singapore, 2025; Volume 1341, pp. 320–329. [CrossRef]

42. Özçelik, Ş.T.; Tek, F.B. Integrating the Focusing Neuron Model with N-BEATS and N-HiTS. In Proceedings of the 9th International Conference on Computer Science and Engineering (UBMK), Antalya, Turkiye, 26–28 October 2024. [CrossRef]
43. Hao, J.; Ma, H.; Sun, F.; Ge, C. N-HiTS Based Tree Barrier Distance Forecasting Method for Enhancing Safety of Electrical Systems. In Proceedings of the 6th International Academic Exchange Conference on Science and Technology Innovation (IAECST), Guangzhou, China, 6–8 December 2024. [CrossRef]
44. Priya, R.Y.; Manjula, R. Enhancing daily streamflow prediction: A comparative analysis of univariate LSTM and N-BEATS models with coupled SWAT-LSTM and SWAT-N-BEATS models incorporating influential SWAT features. *J. Earth Syst. Sci.* **2025**, *134*, 112. [CrossRef]
45. Apte, M.; Haribhakta, Y.V. Advancing Financial Forecasting: A Comparative Analysis of Neural Forecasting Models N-HiTS and N-BEATS. In *Information Systems for Intelligent Systems*; Iglesias, A., Shin, J., Patel, B., Joshi, A., Eds.; Lecture Notes in Networks and Systems; Springer: Singapore, 2025; Volume 1255, pp. 50–63. [CrossRef]
46. Huang, J.; Yan, W.; Li, H.; Hu, S.; Hao, Z.; Li, L.; Lian, X.; Wang, D. Development of two-dimension epidemic prediction model. *Infect. Dis. Model.* **2025**, *10*, 1190–1207. [CrossRef] [PubMed]
47. Ghostine, R.; Gharamti, M.; Hassrouny, S.; Hoteit, I. An Extended SEIR Model with Vaccination for Forecasting the COVID-19 Pandemic in Saudi Arabia Using an Ensemble Kalman Filter. *Mathematics* **2021**, *9*, 636. [CrossRef]
48. Chumachenko, D.; Chumachenko, T.; Meniailov, I.; Muradyan, O.; Zholtkevych, G. Forecasting of COVID-19 Epidemic Process in Ukraine and Neighboring Countries by Gradient Boosting Method. In *Information Technology for Education, Science, and Technics*; Faure, E., Danchenko, O., Bondarenko, M., Tryus, Y., Bazilo, C., Zaspa, G., Eds.; Lecture Notes on Data Engineering and Communications Technologies; Springer: Cham, Switzerland, 2023; Volume 178, pp. 503–514. [CrossRef]
49. Ostus, D.; Hickmann, K.S.; Caragea, P.C.; Higdon, D.; del Valle, S.Y. Forecasting Seasonal Influenza with a State-Space SIR Model. *Ann. Appl. Stat.* **2017**, *11*, 202–224. [CrossRef]
50. Mohanraj, G.; Mohanraj, V.; Marimuthu, M.; Sathiyamoorthi, V.; Ashish, K.L.; Sandeep, K. Epidemic Prediction using Machine Learning and Deep Learning Models on COVID-19 Data. *J. Exp. Theor. Artif. Intell.* **2022**, *35*, 377–393. [CrossRef]
51. Gökgöz, F.; Filiz, F. Deep Learning for Renewable Power Forecasting: An Approach Using LSTM Neural Networks. *Int. J. Energy Power Eng.* **2018**, *12*, 416–420.
52. Chen, Y.H.; Hong, W.-C.; Shen, W.; Huang, N.N. Electric Load Forecasting Based on a Least Squares Support Vector Machine with Fuzzy Time Series and Global Harmony Search Algorithm. *Energies* **2016**, *9*, 70. [CrossRef]
53. Sidenko, I.V.; Atamanyuk, I.; Myroniuk, O.; Kondratenko, G.; Poltorak, A.; Kondratenko, Y. Hybrid neural network and genetic algorithm combination for recognition and avoidance of vehicle obstacles. In Proceedings of the Industrial Simulation Conference 2024, EUROSIS-ETI, Valencia, Spain, 3–5 June 2024.
54. Kondratenko, Y.P.; Shevchenko, A.I. (Eds.) *Research Tendencies and Prospect Domains for AI Development and Implementation*; River Publishers: Gistrup, Denmark, 2024; pp. 1–154.
55. Sidenko, I.; Kondratenko, G.; Heras, O.; Kondratenko, Y. Neural Technologies for Objects Classification with Mobile Applications. *J. Mob. Multimed.* **2024**, *20*, 727–748. [CrossRef]
56. Kondratenko, G.; Sidenko, I.; Saliutin, M.; Kondratenko, Y. Mobile Recognition of Image Components Based on Machine Learning Methods. *J. Mob. Multimed.* **2024**, *20*, 699–726. [CrossRef]
57. Kovaliv, O.; Kondratenko, Y.; Shevchenko, A.; Sidenko, I.; Kondratenko, G. Neural Network Architectures for Recognizing Military Objects on Satellite Images. In Proceedings of the IEEE 12th International Conference on Intelligent Data Acquisition and Advanced Computing Systems: Technology and Applications (IDAACS), Dortmund, Germany, 7–9 September 2023. [CrossRef]
58. Nayak, G.H.H.; Alam, W.; Avinash, G.; Singh, K.N.; Ray, M.; Kumar, R.R. N-BEATS Deep Learning Architecture for Agricultural Commodity Price Forecasting. *Potato Res.* **2025**, *68*, 1437–1457. [CrossRef]
59. Pramanick, N.; Singhal, V.; Neeraj; Mathew, J.; Agarwal, M. Fusion of Wavelet Decomposition and N-BEATS for Improved Stock Market Forecasting. *SN Comput. Sci.* **2024**, *5*, 869. [CrossRef]
60. Ha, T.; Nguyen, P.A.; Vu, T.; Le, N. Federated Learning for Greenhouse Temperature Prediction: A Privacy-Preserving Approach Using N-BEATS. In *Advanced Future Information Technology. FutureTech 2025*; Park, J.S., Wang, J., Pan, Y., Park, J., Eds.; Lecture Notes in Electrical Engineering; Springer: Singapore, 2025; Volume 1483, pp. 102–110. [CrossRef]
61. Sheremet, A.; Kondratenko, Y.; Sidenko, I.; Kondratenko, G. Diagnosis of Lung Disease Based on Medical Images Using Artificial Neural Networks. In Proceedings of the IEEE 3rd Ukraine Conference on Electrical and Computer Engineering (UKRCON), Lviv, Ukraine, 26–28 August 2021. [CrossRef]
62. Sokoliuk, A.; Kondratenko, G.; Sidenko, I.; Kondratenko, Y.; Khomchenko, A.; Atamanyuk, I. Machine Learning Algorithms for Binary Classification of Liver Disease. In Proceedings of the IEEE International Conference on Problems of Infocommunications. Science and Technology (PIC S&T), Kharkiv, Ukraine, 6–9 October 2020. [CrossRef]

63. Kondratenko, Y.; Sidenko, I.; Kondratenko, G.; Petrovych, V.; Taranov, M.; Sova, I. Artificial Neural Networks for Recognition of Brain Tumors on MRI Images. In *Proceedings of the Information and Communication Technologies in Education, Research, and Industrial Applications. ICTERI 2020*; Communications in Computer and Information Science; Springer: Cham, Switzerland, 2020; Volume 1308, pp. 119–140. [CrossRef]
64. Jeffrey, N.; Gunawan, A.A.S.; Kurniawan, A. Development of Multivariate Stock Prediction System Using N-Hits and N-Beats. In *Data Analytics in System Engineering. CoMeSySo 2023*; Silhavy, R., Silhavy, P., Eds.; Lecture Notes in Networks and Systems; Springer: Cham, Switzerland, 2024; Volume 935, pp. 50–63. [CrossRef]
65. Gao, Z.; Zhang, X.; Gao, Z.; Zhou, B.; Liu, Y.; Liu, D.; Ma, X. An Interpretable Hybrid TCN-BiLSTM Model for Reference Evapotranspiration Prediction. *Water Resour. Manage.* **2025**, *39*, 5481–5503. [CrossRef]
66. Xu, C.; Huang, K.; Wei, C.; Wu, X.; Liang, R.; Dong, Y. Landslide Displacement Prediction Based on the VMD–TCN Hybrid Model. *Soil Mech. Found. Eng.* **2025**, *62*, 275–283. [CrossRef]
67. Zhao, L.; Na, Z.; Li, L.; Cui, P. SSA-TCN: Satellite clock offset prediction during outages of RTS stream. *GPS Solut.* **2025**, *29*, 105. [CrossRef]
68. Pradeep Kumar, B.P. A Comparison of CNN, RNN, and FNN Algorithms to Investigate Effective Diabetes Prediction. *Arch. Comput. Methods Eng.* **2025**. [CrossRef]
69. Ben Messaoud, M.A.; Hussein, H. Automatic voice pathology detection and classification using Hamilton product RNN. *Multimed. Tools Appl.* **2025**, *84*, 48977–49004. [CrossRef]
70. Danandeh Mehr, A.; Ghavifekr, A.A.; Ghazaei, E.; Safari, M.J.S.; Ke, C.-Q.; Nourani, V. S-Transformer: A new deep learning model enhanced by sequential transformer encoders for drought forecasting. *Earth Sci. Inform.* **2025**, *18*, 341. [CrossRef]
71. Liu, F.; Nie, L. Light Graph Transformer Model. In *Advancing Recommender Systems with Graph Convolutional Networks*; Springer: Cham, Switzerland, 2025. [CrossRef]
72. Praveenkumar, A.; Jha, G.K.; Madival, S.D.; Lama, A.; Kumar, R.R. Deep Learning Approaches for Potato Price Forecasting: Comparative Analysis of LSTM, Bi-LSTM, and AM-LSTM Models. *Potato Res.* **2025**, *68*, 1941–1963. [CrossRef]
73. Gomolka, Z.; Zeslawska, E.; Czuba, B.; Kondratenko, Y. Diagnosing Dyslexia in Early School-Aged Children Using the LSTM Network and Eye Tracking Technology. *Appl. Sci.* **2024**, *14*, 8004. [CrossRef]
74. Singh, U.; Saurabh, K.; Trehan, N.; Vyas, R.; Vyas, O.P. GA-LSTM: Performance Optimization of LSTM driven Time Series Forecasting. *Comput. Econ.* **2025**, *66*, 2873–2908. [CrossRef]
75. Bai, S.; Kolter, J.Z.; Koltun, V. An Empirical Evaluation of Generic Convolutional and Recurrent Networks for Sequence Modeling. *arXiv* **2018**, arXiv:1803.01271. [CrossRef]
76. Salinas, D.; Flunkert, V.; Gasthaus, J.; Januschowski, T. DeepAR: Probabilistic Forecasting with Autoregressive Recurrent Networks. *Int. J. Forecast.* **2019**, *36*, 1181–1191. [CrossRef]
77. Vaswani, A.; Shazeer, N.; Parmar, N.; Uszkoreit, J.; Jones, L.; Gomez, A.N.; Kaiser, L.; Polosukhin, I. Attention Is All You Need. *arXiv* **2023**, arXiv:1706.03762. [CrossRef]
78. Shazeer, N. GLU Variants Improve Transformer. *arXiv* **2020**, arXiv:2002.05202. [CrossRef]
79. Kim, T.; Kim, J.; Tae, Y.; Park, C.; Choi, J.; Choo, J. Reversible Instance Normalization for Accurate Time-Series Forecasting against Distribution Shift. In Proceedings of the International Conference on Learning Representations (ICLR 2022), Virtual Event, 25–29 April 2022. Available online: https://openreview.net/forum?id=cGDAkQo1C0p (accessed on 18 February 2026).
80. Public Health Center of the Ministry of Health of Ukraine. Infectious Disease in the Population of Ukraine. Available online: https://phc.org.ua/kontrol-zakhvoryuvan/inshi-infekciyni-zakhvoryuvannya/infekciyna-zakhvoryuvanist-naselennya-ukraini (accessed on 24 September 2025).
81. Keesing, F.; Belden, L.K.; Daszak, P.; Dobson, A.; Harvell, C.D.; Holt, R.D.; Hudson, P.; Jolles, A.E.; Jones, K.E.; Mitchell, C.E.; et al. Impacts of Biodiversity on the Emergence and Transmission of Infectious Diseases. *Nature* **2010**, *468*, 647–652. [CrossRef] [PubMed]
82. Schmeller, D.S.; Courchamp, F.; Killeen, G. Biodiversity Loss, Emerging Pathogens and Human Health Risks. *Biodivers. Conserv.* **2020**, *29*, 3095–3102. [CrossRef] [PubMed]
83. Chumachenko, D. Assessing Risks in Infectious Disease Simulation Models for Emergency Setting. In *Developments in Information and Knowledge Management Systems for Business Applications*; Štarchoň, P., Fedushko, S., Gubíniova, K., Eds.; Studies in Systems, Decision and Control; Springer: Cham, Switzerland, 2026; Volume 602, pp. 445–478. [CrossRef]
84. Zbezhkhovska, U.; Chumachenko, D. Smoothing Techniques for Improving COVID-19 Time Series Forecasting Across Countries. *Computation* **2025**, *13*, 136. [CrossRef]
85. Chumachenko, D.; Bazilevych, K.; Butkevych, M.; Meniailov, I.; Parfeniuk, Y.; Sidenko, I.; Chumachenko, T. Methodology for assessing the impact of emergencies on the spread of infectious diseases. *Radioelectron. Comput. Syst.* **2024**, *3*, 6–26. [CrossRef]
86. Luppichini, M.; Bini, M.; Giannecchini, R. CleverRiver: An open source and free Google Colab toolkit for deep-learning river-flow models. *Earth Sci. Inform.* **2023**, *16*, 1119–1130. [CrossRef]

87. Rawat, R. Optimizing ML models for cybercrime detection: Balancing performance, energy consumption, and carbon footprint through multi-objective optimization. *Discov. Artif. Intell.* **2025**, *5*, 38. [CrossRef]
88. Hoseini, F.; Notash, A.Y. Image captioning using bidirectional LSTM neural network. *Discov. Artif. Intell.* **2025**, *5*, 80. [CrossRef]
89. Atif, D. Enhancing Long-Term GDP Forecasting with Advanced Hybrid Models: A Comparative Study of ARIMA-LSTM and ARIMA-TCN with Dense Regression. *Comput. Econ.* **2025**, *65*, 3447–3473. [CrossRef]
90. Singh, A.; Tripathi, T.; Ranjan, R.; Tiwari, A.K. Time series forecasting of infant mortality rate in India using Bayesian ARIMA models. *BMC Public Health* **2025**, *25*, 2855. [CrossRef] [PubMed]
91. Liu, J.; Zhang, Z.; Lyu, B.; Feng, R.; He, Y. A hybrid ARIMA-BP approach for superior accuracy in predicting traffic accident losses. *Sci. Rep.* **2025**, *15*, 24328. [CrossRef]
92. Samal, U.; Kumar, A. Improving software reliability: A hybrid ARIMA-LSTM approach for fault prediction. *Int. J. Syst. Assur. Eng. Manag.* **2025**, *16*, 1757–1769. [CrossRef]
93. Time Series Made Easy in Python. Available online: https://unit8co.github.io/darts/index.html (accessed on 10 October 2025).
94. Sova, I.; Sidenko, I.; Kondratenko, Y. Machine Learning Technology for Neoplasm Segmentation on Brain MRI Scans. In *CEUR Workshop Proceedings*; CEUR-WS: Aachen, Germany, 2020; Volume 2791, pp. 50–59. Available online: https://ceur-ws.org/Vol-2791/2020200050.pdf (accessed on 18 February 2026).
95. Khortiuk, I.; Kondratenko, G.V.; Sidenko, I.V.; Kondratenko, Y.P. Scoring system based on neural networks for identification of factors in image perception. In *CEUR Workshop Proceedings*; CEUR-WS: Aachen, Germany, 2020; Volume 2604, pp. 993–1003.
96. Sidenko, I.; Filina, K.; Kondratenko, G.; Chabanovskyi, D.; Kondratenko, Y. Eye-tracking technology for the analysis of dynamic data. In Proceedings of the IEEE 9th International Conference on Dependable Systems, Services and Technologies (DESSERT), Kyiv, Ukraine, 24–27 May 2018. [CrossRef]
97. Sidenko, I.; Trukhov, A.; Kondratenko, G.; Zhukov, Y.; Kondratenko, Y. Machine Learning for Unmanned Aerial Vehicle Routing on Rough Terrain. In *Advances in Computer Science for Engineering and Education VI. ICCSEEA 2023*; Hu, Z., Dychka, I., He, M., Eds.; Lecture Notes on Data Engineering and Communications Technologies; Springer: Cham, Switzerland, 2023; Volume 181, pp. 626–635. [CrossRef]
98. Zinchenko, V.; Kondratenko, G.; Sidenko, I.; Kondratenko, Y. Computer Vision in Control and Optimization of Road Traffic. In Proceedings of the IEEE Third International Conference on Data Stream Mining & Processing (DSMP), Lviv, Ukraine, 21–25 August 2020. [CrossRef]
99. Leizerovych, R.; Kondratenko, G.; Sidenko, I.; Kondratenko, Y. IoT-complex for Monitoring and Analysis of Motor Highway Condition Using Artificial Neural Networks. In Proceedings of the IEEE 11th International Conference on Dependable Systems, Services and Technologies (DESSERT), Kyiv, Ukraine, 14–18 May 2020. [CrossRef]
100. Kondratenko, Y.P.; Kuntsevich, V.M.; Chikrii, A.A.; Gubarev, V.F. (Eds.) *Advanced Control Systems: Theory and Applications*; River Publishers: Gistrup, Denmark, 2021; pp. 1–441. [CrossRef]
101. Ivanova, K.; Kondratenko, G.V.; Sidenko, I.V.; Kondratenko, Y.P. Artificial intelligence in automated system for web-interfaces visual testing. In *CEUR Workshop Proceedings*; CEUR-WS: Aachen, Germany, 2020; Volume 2604, pp. 1019–1031. Available online: https://ceur-ws.org/Vol-2604/paper68.pdf (accessed on 18 February 2026).
102. Kondratenko, Y.P.; Kuntsevich, V.M.; Chikrii, A.A.; Gubarev, V.F. (Eds.) *Recent Developments in Automatic Control Systems*; River Publishers: Gistrup, Denmark, 2022; pp. 1–492.
103. Kondratenko, Y.; Shevchenko, A.; Zhukov, Y.; Kondratenko, G.; Striuk, O. Tendencies and Challenges of Artificial Intelligence Development and Implementation. In Proceedings of the IEEE 12th International Conference on Intelligent Data Acquisition and Advanced Computing Systems: Technology and Applications (IDAACS), Dortmund, Germany, 7–9 September 2023. [CrossRef]
104. Striuk, O.; Kondratenko, Y. Implementation of Generative Adversarial Networks in Mobile Applications for Image Data Enhancement. *J. Mob. Multimed.* **2023**, *19*, 823–838. [CrossRef]
105. Kondratenko, Y.P.; Kondratenkob, G.; Shevchenkoa, A.; Slyusara, V.; Zhukovc, Y.; Vakulenkoa, M. Towards Implementing the Strategy of Artificial Intelligence Development: Ukraine Peculiarities. In *CEUR Workshop Proceedings*; CEUR-WS: Aachen, Germany, 2023; Volume 3513, pp. 106–117. Available online: https://ceur-ws.org/Vol-3513/paper09.pdf (accessed on 18 February 2026).
106. Tetyana, M.; Kondratenko, Y.; Sidenko, I.; Kondratenko, G. Computer Vision Mobile System for Education Using Augmented Reality Technology. *J. Mob. Multimed.* **2021**, *17*, 555–576. [CrossRef]
107. de Myttenaere, B.; Golden, B.; Le Grand, F.; Rossi, F. Mean Absolute Percentage Error for Regression Models. *Neurocomputing* **2016**, *192*, 38–48. [CrossRef]
108. Dekking, F.M.; Kraaikamp, C.; Lopuhaä, H.P.; Meester, L.E. *A Modern Introduction to Probability and Statistics*; Springer: London, UK, 2005. [CrossRef]
109. Marou, V.; Vardavas, C.I.; Aslanoglou, K.; Nikitara, K.; Plyta, Z.; Leonardi-Bee, J.; Atkins, K.; Condell, O.; Lamb, F.; Suk, J.E. The Impact of Conflict on Infectious Disease: A Systematic Literature Review. *Confl. Health* **2024**, *18*, 27. [CrossRef]
110. Kannan, A.; Chen, R.; Akhtar, Z.; Sutton, B.; Quigley, A.; Morris, M.J.; MacIntyre, C.R. Use of Open-Source Epidemic Intelligence for Infectious Disease Outbreaks, Ukraine, 2022. *Emerg. Infect. Dis.* **2024**, *30*, 1865–1871. [CrossRef]

111. Oreshkin, B.N.; Carpov, D.; Chapados, N.; Bengio, Y. N-BEATS: Neural Basis Expansion Analysis for Interpretable Time Series Forecasting. Available online: https://arxiv.org/abs/1905.10437 (accessed on 18 February 2026).
112. Wang, Y.; Smola, A.; Maddix, D.; Gasthaus, J.; Foster, D.; Januschowski, T. Deep Factors for Forecasting. In Proceedings of the 36th International Conference on Machine Learning, PMLR 97, 2019, Long Beach, CA, USA, 9–15 June 2019.
113. Chen, H.; Rossi, R.A.; Mahadik, K.; Kim, S.; Eldardiry, H. Graph Deep Factors for Probabilistic Time-Series Forecasting. *ACM Trans. Knowl. Discov. Data* **2022**, *17*, 26. [CrossRef]
114. Lim, B.; Arık, S.Ö.; Loeff, N.; Pfister, T. Temporal Fusion Transformers for Interpretable Multi-Horizon Time Series Forecasting. *Int. J. Forecast.* **2021**, *37*, 1748–1764. [CrossRef]
115. Zhou, H.; Zhang, S.; Peng, J.; Zhang, S.; Li, J.; Xiong, H.; Zhang, W. Informer: Beyond Efficient Transformer for Long Sequence Time-Series Forecasting. *Proc. AAAI Conf. Artif. Intell.* **2021**, *35*, 11106–11115. [CrossRef]
116. Wu, H.; Xu, J.; Wang, J.; Long, M. Autoformer: Decomposition Transformers with Auto-Correlation for Long-Term Series Forecasting. In Proceedings of the 35th International Conference on Neural Information Processing Systems, NIPS'21, Online, 6–14 December 2021; pp. 22419–22430.
117. Zhou, T.; Ma, Z.; Wen, Q.; Wang, X.; Sun, L.; Jin, R. FEDformer: Frequency Enhanced Decomposed Transformer for Long-Term Series Forecasting. In Proceedings of the International conference on machine learning, Seoul, Republic of Korea, 7–9 July 2022.
118. McGough, S.F.; Johansson, M.A.; Lipsitch, M.; Menzies, N.A. Nowcasting by Bayesian Smoothing: A Flexible, Generalizable Model for Real-Time Epidemic Tracking. *PLoS Comput. Biol.* **2020**, *16*, e1007735. [CrossRef] [PubMed]